Online System Identification of DC-DC Converter for RFPA

Ahmed Lashin [1*] Ahmed Mahfouz [2]
1.Egyptian Space Program, NARSS, 23 Joseph Tito street, El-Nozha El-Gedida, Cairo, Egypt
2.Electrical Power Engineering Department, Faculty of Engineering, Cairo University, Egypt
* E-mail of the corresponding author: a.s.lashin@narss.sci.eg

Abstract
This paper describes non-parametric system identification of a DC-DC converter based on spectral analysis correlation method. The used technique identifies the open-loop characteristics of a DC-DC converter online while the unit operates in closed-loop. A digital controller is used to perform both the closed-loop control of the converter and to periodically identify the converter by injecting a pseudo-random binary perturbation. Experimental results are provided for an example buck-boost converter to demonstrate accurate identification of the converter control-to-output frequency response. Experimental results have revealed stable operation of the converter during identification while meeting severe transient response requirements. This technique is advantageous for developing wide-input range/wide-output range converters which are vital for RF power amplifiers used in space and telecommunication applications.
Keywords: System Identification, Adaptive Control, DC-DC converter, RFPA

1. Introduction

In space and telecommunication applications there has been an increasing demand of DC-DC converters which can supply programmable output voltages to loads while being fed from a widely unregulated input (Hurtz & Sugasawara, 2003) (Kankam & Elbuluk, 2001). Typical example of the wide-input range/wide-output range converters are solar arrays maximum power point tracker (MPPT) and power supply of RF power amplifier (RFPA) (Sahu, 2004) (Vahid Yousefzadeh, Narisi Wang, Zoya Popović and Dragan Maksimović, 2006) (Steyaert, van Roermund, & Casier, 2009) (Maxim-IC, 2005).

Models of DC-DC converter has shown that its transfer function is dependent on its input voltage, duty cycle and load current, which suggests that the DC-DC converter design is related to a narrow range of operating points. Working on a wide-range of operating points may cause the converter to behave unstably. As the converter is a nonlinear system whose transfer function varies by changing the operating point, the controller needs to be modified to adapt for the changes of the converter. As shown in Figure 1 , an adaptive controller operation has two stages (Miao, Zane, & Maksimović, 2005):

1. System identification stage. Here, the frequency response of the converter's control-to-output transfer function is measured by non-parametric system identification.
2. The controller design stage, in which the PID parameters are modified to adapt for the changes in the DC-DC converter.

System identification is categorized into parametric and non-parametric methods (Ljung, 1999). In parametric identification, a system model is assumed, and the identification tries to estimate of the model parameters. In non-parametric identification, the system frequency response is computed directly. Nonparametric methods include correlation analysis, transient-response analysis, and frequency response, Fourier, or spectrum analysis (Ljung, 1999) (Aström & Wittenmark, 1995).

In this paper we focus on non-parametric identification based on correlation method with the objective of calculating system frequency response online while the converter works in close-loop

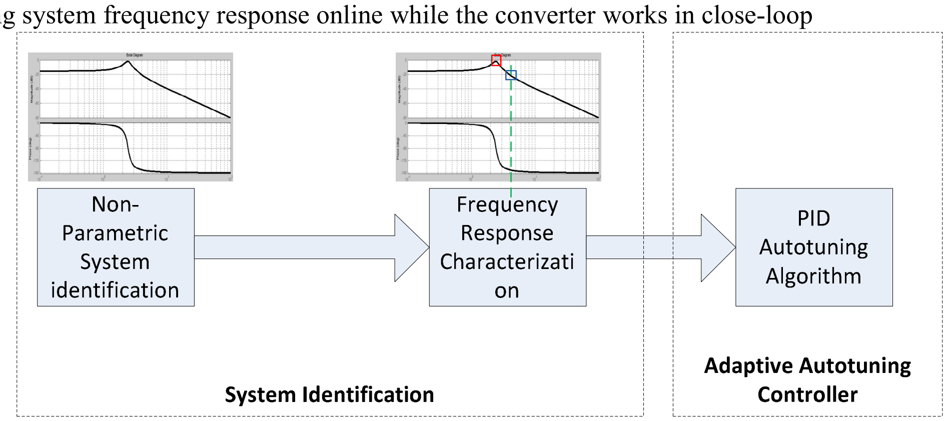

Figure 1. Block Diagram of Adaptive Controller

2. SPECTRAL ANALYSIS METHOD

A DC-DC converter is non-linear system whose transfer function is dependent on its inputs (Erickson & Maksimović, 2001). However, at a certain operating point, the DC-DC converter can be modelled as a linear time-invariant (LTI) discrete-time system that can be described by (Rahman, Parayandeh, Wang, & Prodić, June 2006) (Maksimović, May 2002.)

$$y[n] = \sum_{k=-\infty}^{\infty} h[k]x[n-k] = h[n] \otimes x[n] \tag{1}$$

Where, *x[n]*, *y[n]* and *h[k]* are the input signal, the output signal and the system impulse response respectively. The *cross-correlation sequence* $r_{xy}[l]$ of two signals *x[n]* and *y[n]* is given by

$$r_{xy}[l] = \sum_{n=-\infty}^{\infty} y[n]x[n-l] \ , \ l = \pm 1, \pm 2, \pm 3, \ldots \tag{2}$$

From (1) and (2),

$$r_{xy}[l] = \sum_{n=-\infty}^{\infty} \left(\sum_{k=-\infty}^{\infty} x[n-k]h[k] \right) x[n-l] \tag{3}$$

By exchanging the summations,

$$r_{xy}[l] = \sum_{k=-\infty}^{\infty} h[k] \left(\sum_{n=-\infty}^{\infty} x[n-k]x[n-l] \right) \tag{4}$$

Accordingly,

$$r_{yx}[l] = \sum_{k=-\infty}^{\infty} h[k] r_{xx}[l-k] \tag{5}$$

Where, $r_{xx}[l]$ is the auto-correlation sequence of the signal *x[n]*.
Using Parseval's Relation and Wiener-Khinchin theorem in calculating DTFT of the above Equation we get (Ljung, 1999):

$$S_{yx}(e^{j\omega}) = H(e^{j\omega}) S_{xx}(e^{j\omega}) \tag{6}$$

$$\boxed{H(e^{j\omega}) = \frac{S_{xy}(e^{j\omega})}{S_{xx}(e^{j\omega})} = \frac{DTFT(r_{yx}[l])}{DTFT(r_{xx}[l])}} \tag{7}$$

Where, $S_{xx}(e^{j\omega})$, $S_{yx}(e^{j\omega})$,) and $H(e^{j\omega})$ are *energy density spectrum of x[n],* the *cross energy density spectrum* and the *system frequency response* respectively.
In other words, if the auto-correlation of the input $r_{xx}[l]$ is an ideal delta function $\delta[l]$, then the DTFT of cross-corrleation of the input-output is the frequency response of the system.

3. White Noise

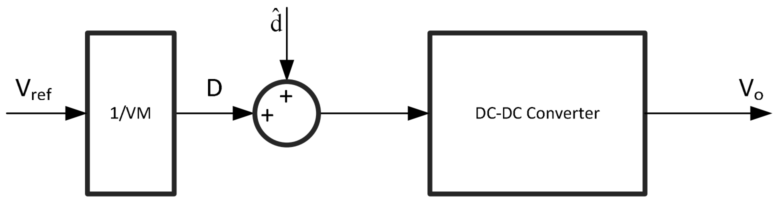

Figure 1. Open-loop identification of DC-DC converter

Figure 1, shows a typical system identification of an open-loop converter control-to output transfer function by injecting white noise in the duty cycle.

Ideal white noise required for equation 错误!未找到引用源。is impossible to be implemented as it needs infinite samples. Therefore we can make a compromise by using pseudo random binary sequence (PRBS) perturbations instead. The PRBS is periodic and deterministic. The data length for one period of an n-bit maximum length PRBS is given by: $m=2^n-1$. The maximum length sequence (MLS) of the PRBS has the best properties for identification. There is a trade-off on the selection of m while achieving best frequency sampling and resolution. The start and stop of the effective frequency sweep is given by $f_0/2$ and f_0/m respectively, where f_0 is the PRBS frequency. Besides, the frequency resolution or spacing between frequency samples is f_0/m. Thus, f_0 must be sufficiently high to reach the desired high frequency content, while f_0/m must be sufficiently small to reach low frequency content and to achieve good frequency resolution.

Another constraint is that the sampling window of a single PRBS period in the time domain, given by m/f_0. must be sufficiently longer than the system settling time. In addition, PRBS magnitude should be carefully selected proportionally to the settling time of the system so as to ensure proper DPWM operation and to keep the output voltage within the limits during the identification period.

4. Closed-loop identification

In order to identify the converter's transfer function without disrupting its closed loop-operation., the error signal V_e must be simulated during identification period. By latching the error to its previous value we prevent a sudden change of the output voltage. Because the error changes repeatedly over the switching period, we latch a queue of error values before the identification and we retrieve this queue during identification period. The compensator must be disconnected during identification.

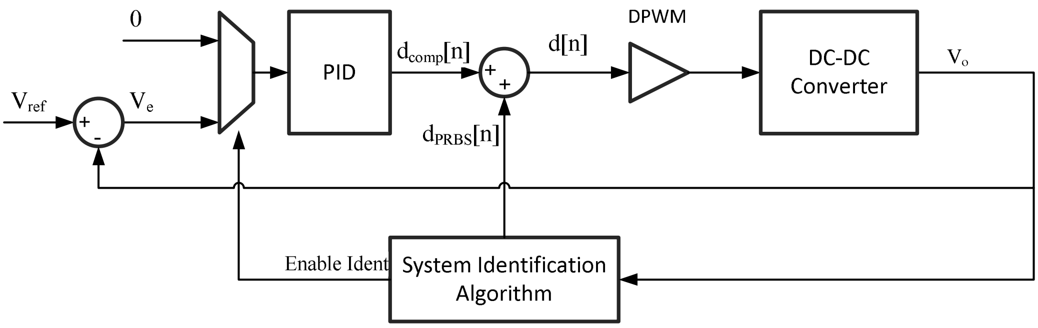

Figure 2. Block Diagram of closed-loop system identification

5. Identification example: buck-boost converter

Figure 3 shows a buck-boost converter used to supply an RF power amplifier (RFPA). The output RF power range is 5 to 20 dBm which indicates that the output voltage range is V_o = -0.01778…-1V . The converter input voltage range is V_g = 2..6V. The RFPA is simulated by a 10 Ω load.

The converter switching frequency and the sampling frequency are set to 1MHz.

The PRBS was injected only during steady-state operation. The converter was designed to work in continuous conduction mode during the identification phase and the output voltage ripple should not exceed 50mv. Therefore the following values were selected for the output filter .C = 2 µF, L= 10 µH.

5.1 Small Signal Model

By means of *small ripple approximation* we can create a linearized averaged model of the buck-boost converter shown in Figure 3.

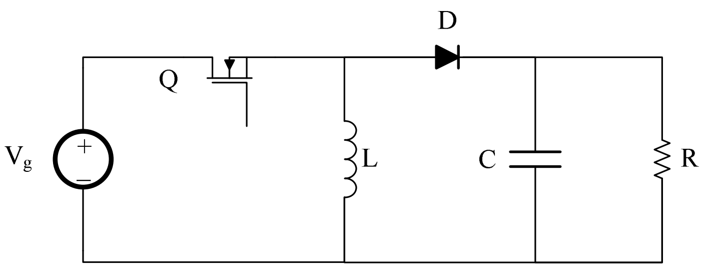

Figure 3. Buck-boost converter circuit

Using the inductor *volt-second balance* and *capacitor charge-balance* principles (Erickson & Maksimović, 2001), we can extract the following equations:

$$\langle v_L(t)\rangle_{T_s} = D(V_g + \hat{v}_g(t)) - (DR_{on} + R_L + D'R_D)(I + \hat{i}_L(t)) + (V_g + I[R_D - R_{on}] + V_D - V_o)\hat{d}(t) - D'V_D + D'(V_o + \hat{v}_o(t)) \quad (8)$$

$$\langle i_C(t)\rangle_{T_s} = \frac{-(V_o + \hat{v}_o(t))}{R} - D'(I + \hat{i}_L(t)) + I\hat{d}(t) \quad (9)$$

$$I_g + \hat{i}_g(t) = D(I + \hat{i}_L(t)) + I\hat{d}(t) \quad (10)$$

Hence, we can construct the small-signal AC model of the system:

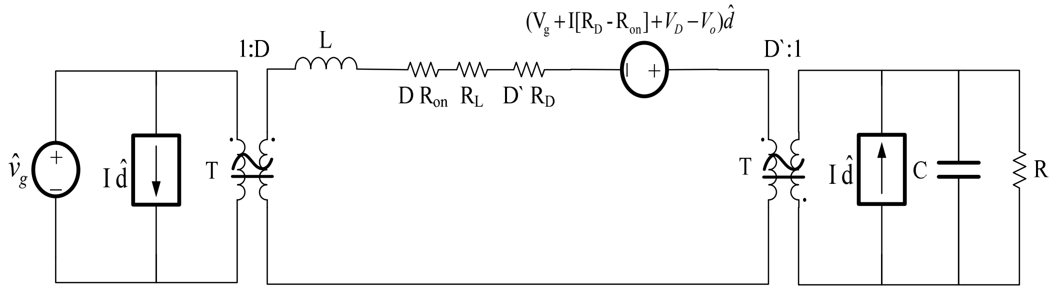

Figure 4. Small-signal AC model of the buck-boost converter

It can be inferred from the above circuit that the control-to-output transfer function G_{vd} of an ideal converter is given by:

$$G_{vd} = G_{d0}\frac{1 - \frac{s}{\omega_z}}{\frac{s^2}{\omega_0^2} + \frac{s}{Q\omega_0} + 1} \quad (11)$$

Where the system salient features are: $G_{d0}=V_o/(DD`)$ , $\omega_0=D/\surd(LC)$, $\omega_z=D`^2R/(DL)$ and $Q=D`R\surd(C/L)$.

5.2 System Block Diagram

Spectral analysis technique is used. A pseudorandom small perturbation is injected in the duty cycle. The following figure shows the system block diagram used for buck-boost system identification.

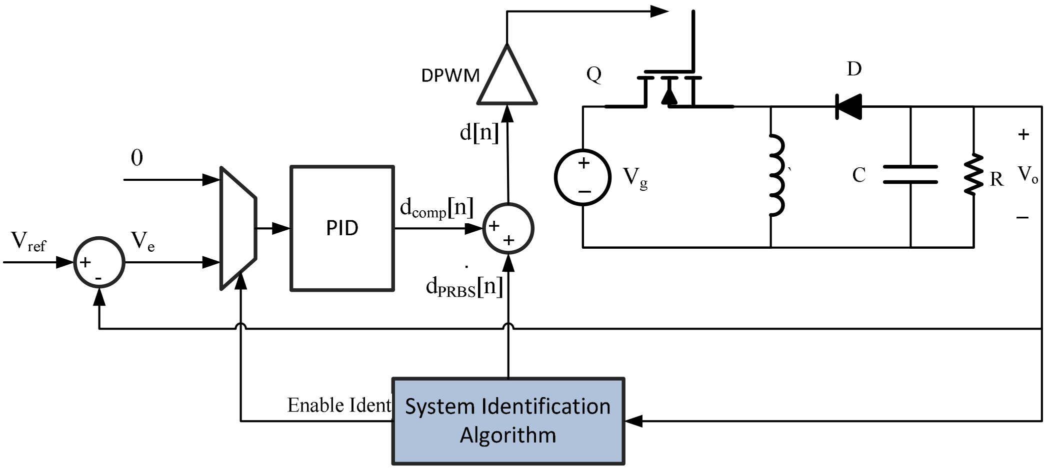

Figure 5. System block Diagram

An umbilical PID compensator was created in order to ensure system stability over the whole operation range. The compensator transfer function is:

$$G_C = G_{PID} \frac{\left(1+\frac{\omega_L}{s}\right)\left(1+\frac{s}{\omega_{zz}}\right)}{\left(1+\frac{s}{\omega_P}\right)} \quad (12)$$

Where, ω_L , ω_{zz} and ω_p are the PI inverted zero, PD lead compensator, PD lag compensator, frequencies respectively.

Table 1 - PID parameters for selected cases

Case	V_g (volt)	V_o (volt)	G_{PID} (db)	ω_{zz} (rad/sec)	ω_L (rad/sec)	ω_P (rad/sec)
1	2	-0.1778	15.69	-2.58E+05	-7.86E+04	-1.27E+06
2	2	-1	26.61	-1.81E+05	-8.62E+04	-2.26E+06
3	3	-0.1778	15.26	-2.55E+05	-7.93E+04	-1.72E+06
4	3	-1	19.31	-2.10E+05	-9.71E+04	-2.63E+06
5	4	-0.1778	65.55	-3.10E+05	-6.29E+04	-7.57E+06
6	4	-1	16.33	-2.23E+05	-8.62E+04	-3.14E+06
7	5	-0.1778	91.31	-2.73E+05	-1.51E+05	-2.49E+07
8	5	-1	21.33	-2.59E+05	-8.12E+04	-4.48E+06
9	6	-0.1778	9.30	-2.73E+05	-1.53E+05	-2.65E+06
10	6	-1	21.77	-2.32E+05	-6.40E+04	-5.36E+06

The above table summarizes the PID parameters used for each operating point.

5.3 PRBS Input signal

The requirements for practical system identification include:

a. Signal injection should not disturb normal system operation in terms of static and dynamic voltage regulation.
b. The identification should be immune to switching and quantization noise.

The system was perturbed by an 11-bit PRBS input signal. The PRBS was injected as shown in Figure 5. The frequency of the PRBS is equivalent to the switching frequency of the converter.

The 11-bit MLS PRBS signal was generated using the Modulo-2 equation *u(t)=rem(A(q)u(t),2)*. Where, *A(q)* is the polynomial $q^{11}+q^9+1$ (Ljung, 1999). The PRBS signal magnitude is 1% of steady-state compensated duty cycle.

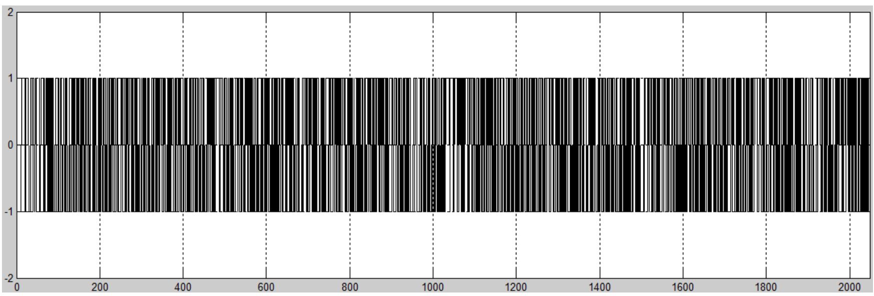

Figure 6. 11-bit PRBS input signal

As shown in Figure 7, the auto-correlation of the PRBS is very close to a delta function.

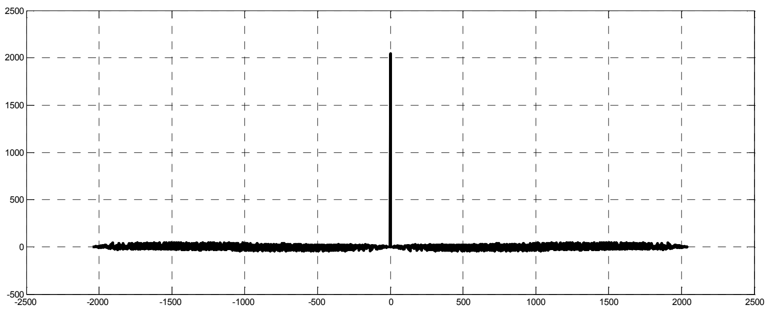

Figure 7. Cross-correlation of an 11-bit PRBS input signal

5.4 Output Transient Response

Figure 8 and Figure 9 show that during identification period the converter output voltage ripple didn't exceed 50 mv and the inductor current didn't exceed 50% of its steady state value. *i.e.* The converter kept working in continuous conduction mode.

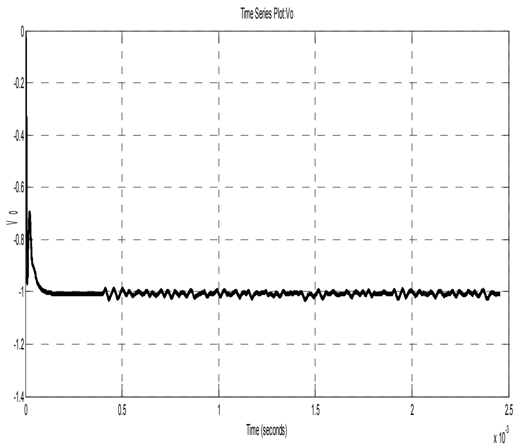

Figure 8. Output Voltage during Identification of case 2

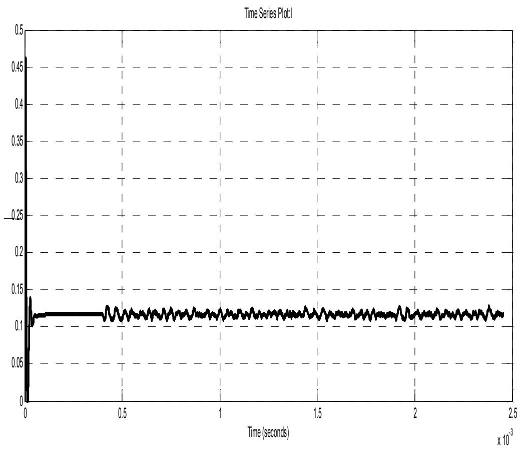

Figure 9. Inductor Current during Identification of case 2

5.5 Output Frequency Response

The cross-correlation of the input and output is calculated. The DTFT of the cross-correlation represents the frequency response of the system. Figure 10 shows a comparison between identified control-to-output frequency response (dotted line) and the frequency response of G_{vd} calculated in section 5.1 (solid line) for case 2 of Table 1.

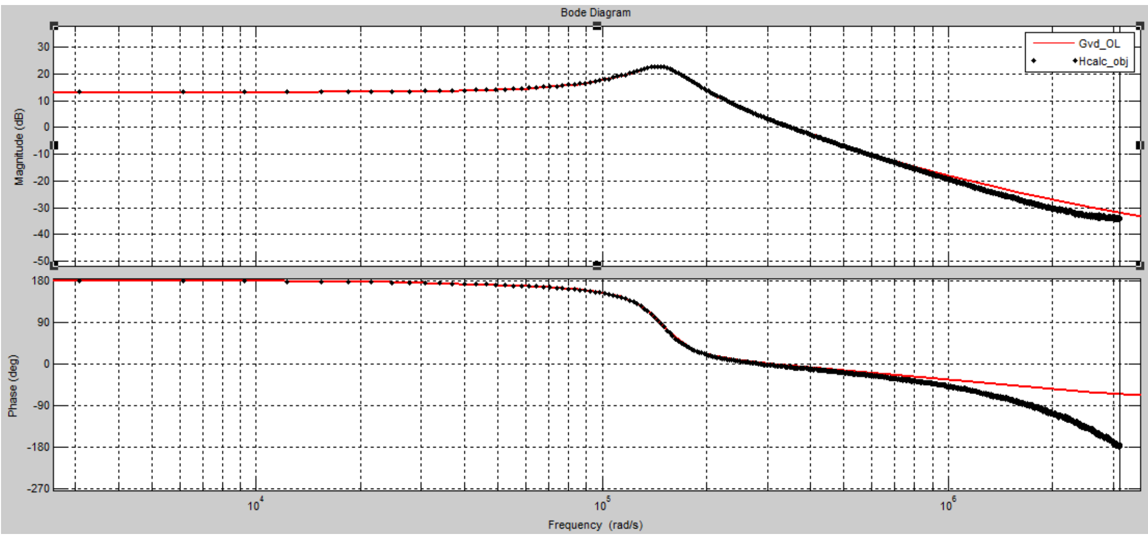

Figure 10. Case 2: Frequency response of open-loop G_{vd}: solid line calculated – dotted line identified.

6. Conclusions and future research

In this Paper we have demonstrated a realistic approach for online identification of the open-loop characteristics of a DC-DC converter which works in closed-loop. The identification parameters kept stable operation of the converter while obeying sever transient response limitations. During identification period the feedback error signal was simulated to its previous steady-state value. The cross-correlation between input and output was calculated and the frequency response was identified accurately for a 5-to-20dbm RF power amplifier DC-DC converter. As referred in section, by building a self-tuning regulator, the results of this paper can be used in building a complete adaptive control system of the DC-DC converter with the objective of achieving wide input / wide output range.

References

Aström, K.J. & Wittenmark, B., (1995). *Adaptive control*. 2nd ed. Addison – Wesley.

Erickson, R.W. & Maksimović, D., (2001). *Fundamentals of Power Electronics*. Second Edition ed. Norwell, Mass.: Kluwer Academic Publishers.
Hurtz, G. & Sugasawara, D., (2003). CDMA handset design challenge: 11 separate power supplies. *Commzmication Design-An EE Times Publication*.
Kankam, M.D. & Elbuluk, M.E., (2001). A Survey of Power Electronics Applications in Aerospace technologies. In *36th Intersociety Energy Conversion Engineering Conference*. Savannah, Georgia , USA.
Ljung, L., (1999). *System Identification: Theory for the User*. 2nd ed. Upper Saddle River, N.J.: Prentice- Hall.
Maksimović, D., (2002). Power management model and implementation of power management ICs for next generation wireless applications. Phoenix, May 2002. tutorial presented at the IEEE Symposium on Circuits and Systems, ISCAS'02.
Maxim-IC, (2005). Application Note 3434: RF Power Reduction for CDMA/WCDMA Cellular Phones.
Miao, B., Zane, R. & Maksimović, D., (2005). Automated Digital Controller Design for Switching Converters. In *Power Electronics specialists conference PESC*. Recife, Brazil, (2005).
Rahman, N., Parayandeh, A., Wang, K. & Prodić, A., (2006). Multimode Digital SMPS Controller IC for Low-Power Management. In *Proc. IEEE International Symposium on Circuits and Systems (ISCAS)*. Kos, Greece, (June 2006).
Sahu, B., (2004). Integrated, Dynamically Adaptive Supplies for Linear RF Power Amplifiers in Portable Applications. *PhD Dissertion*.
Steyaert, M., van Roermund, A.H.M. & Casier, H., (2009). *Analog Circuit Design: High-speed Clock and Data Recovery, High-performance Amplifiers, Power Management*. Springer.
Vahid Yousefzadeh, Narisi Wang, Zoya Popović and Dragan Maksimović, (2006). A Digitally Controlled DC/DC Converter for an RF Power Amplifier. *IEEE Transactions on Power Electronics*.